Role of an Artificial Neural Network and a Wavelet Transform for Condition Monitoring of the Combined Faults of Unbalance and Cracked Rotors

H. K. Srinivas

Department of Mechanical Engineering, P.E.S. College of Engineering, Mandya, Karnataka, India

K. S. Srinivasan

EIT, Ummathur, Chamarajanagar Dist, Karnataka, India

K. N. Umesh

Department of Mechanical Engineering, PESCE, Mandya, Karnataka, India

(Received 26 August 2009; revised 2 March 2010; accepted 26 April 2010)

The vibration analysis of rotating machinery indicates the condition of potential faults such as unbalance, bent shaft, shaft crack, bearing clearance, rotor rub, misalignment, looseness, oil whirl and whip, and other malfunctions. More than one fault can occur in a rotor. This paper describes the application of an artificial neural network (ANN) and wavelet transform (WT) for the prediction of the effect of the combined faults of unbalance and shaft crack on the frequency components of the vibration signature of the rotating machinery. The experimental data of the frequency components and the corresponding root mean square (RMS) velocity (amplitude) data are used as inputs to train the ANN, which consists of a three-layered network. The ANN is trained using an improved multilayer feed forward back propagation Levenberg-Marquardt algorithm. In particular, the overall success rates achieved were 99.78% for unbalance, 99.81% for shaft crack, and 99.45% for the combined faults of unbalance and shaft crack. The wavelet transform approach enables instant to instant observation of different frequency components over the full spectrum. A new technique combining the WT with ANN performs three general tasks: data acquisition, feature extraction, and fault identification. This method is tested successfully for the individual and combined faults of unbalance and shaft crack at a success rate of 99.9%.

1. INTRODUCTION

In order to avoid the failure of various types of rotating machinery, including mechanical and electrical ones, using sophisticated instrumentation to monitor the conditions of various machine signatures has been found to be of considerable use. Vibration measurement and analysis has been applied with success[1] to machines such as steam and gas turbines, pumps, compressors, and induction motors. Faults such as unbalance, misalignment, looseness, rub, and cracks, generate vibration signals. In the present work, an experimental study has been carried out for a steady state response (constant speed of 1500 rpm) of the rotor for different unbalance masses and cracks on the rotor test rig. The vibration frequency components recorded in the horizontal, vertical, and axial directions for the analysis are applied. The experimental study has also been carried out to discover the difference in vibration characteristics due to the combined faults of unbalance and crack growth. The monitoring of the vibration of rotating machines has been reported as being a useful technique for the analysis of their condition.[2–5] Vibration condition monitoring as an aid to fault diagnosis is examined by Taylor (1995). Smalley and colleagues (1996) present a method of assessing the severity of vibrations in terms of the probability of damage by analyzing the vibration signals. Though the measured vibration signatures of frequency domain features are adequate to identify the faults, there is a need for a reliable, fast, and automated procedure of obtaining diagnostics.[6] Unbalance is an important cause of vibration in rotating machinery, and the reduction of such vibration by balancing needs attention. In this paper, the experimental studies are presented in the dynamic balancing of a flexible shaft using the four run method (FRM) (Mallik & Basu). The vibration frequency of rotor unbalance is synchronous, i.e., one time the shaft rotation speed (1X rpm). Rotor unbalance has been reported to appear occasionally in the frequency domain as a series of harmonics of the shaft running speed, i.e., 1X rpm, 2X rpm, 3X rpm, 4X rpm, etc[7] induction motors, etc.

1.1. Artificial Neural Networks

The neural network techniques are used in conjunction with signal analysis techniques for the classification and quantification of faults in some applications.[8] Kaminski has developed neural networks to identify the approximate location of damage due to cracks through the analysis of changes in the neural frequencies.[9] McCormick and Nandi use a neural network method for automatically classifying the machine condition from the vibration time series.[10] Vyas and Satish Kumar have carried out experimental studies to generate data for rotating machinery faults such as mass unbalance and bearing cap loose.[11] Srinivasan has carried out extensive studies on faults such as parallel misalignment, angular misalignment, unbalance, crack, light and heavy rubs, looseness, and bearing

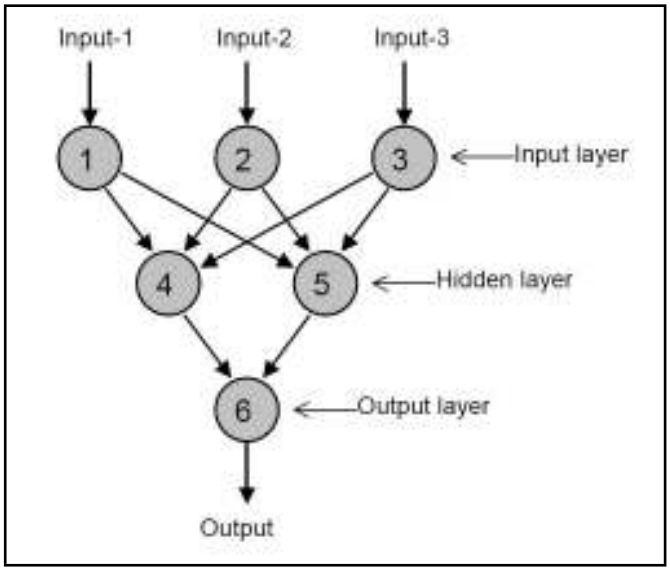

Figure 1. Three layers network.

clearance.[12]

Figure 1 shows a simple network consisting of three layers with one input layer, one hidden layer and one output layer. There are no connections between nodes in the same layer and no connections that bridge the layers. Such networks with only one hidden layer can uniformly approximate any continuous function and therefore provide a theoretical basis for the use of this type of network. The input-output relationship of each node is determined by a set of connection weights Wi, a threshold parameter bi, and a node activation function $A(\ )$ such that

$$Y = A(WiXi + bi), \tag{1}$$

where Y is the output of the node and Xi are the inputs. The activation function $A(\ )$ defines the output of a neuron in terms of activity level at its input. The sigmoid function is the most common activation function used in neural networks. It is defined as a strictly increasing function that exhibits smoothness and asymptotic properties. The Tan-sigmoid activation function is used in the hidden layer. The purelin activation function is used in the output layer.

In the present work, an improved back propagation neural network has been applied for the diagnosis of the combined faults of unbalance and shaft bow. It attempts to minimize the square of the error between the output of the network and the desired outputs by changing the connection weights that use some form of gradient descent. The back propagation method has used gradient descent techniques, which are simply the techniques, where parameters such as weights and biases are moved in the opposite direction towards the error gradient. The Levenberg-Marquardt algorithm has the best convergence speeds for small and medium size networks.[13,14] This optimization technique is more accurate and faster than the gradient descent method. The Levenberg-Marquardt update rule is

$$\Delta W = (J^T J + \mu I)^{-1} J^T e, \tag{2}$$

where ΔW is the small change in weight. J is the n by m Jacobian matrix $J^T J$ which keeps the function N rows of J linearly independent, and μ is a small positive constant chosen to ensure $(J^T J + \mu I)$ is positive for all n values. If μ is very large, the above expression approximates gradient descent; if it is small, the above expression becomes the Gauss-Newton method. The Gauss-Newton method is faster, more accurate, and near an error minimum. Training continues until the error goal is met, the minimum error gradient occurs, the maximum value of μ occurs, or the maximum number of epochs has been finished. The MATLAB Neural Network Toolbox has been applied for diagnosing the rotating machinery faults.

1.2. Wavelet Transform

The wavelet transforms acts as a "mathematical microscope" in which one can observe different paths of the signal by "adjusting the focus". A frequency component of the RMS velocity indicates the health of a particular machine. The wavelet transform approach allows the detection of short-lived frequency component in the signals. The method is logical since high-frequency components (such as short bursts) need high-frequency resolution as compared with low-frequency components, which require low-frequency resolution. This paper also describes the use of wavelet transform to decompose the vibration signal into several frequency ranges at different levels of resolution. The strength (RMS) of the selected decomposed signals is then calculated under the combined faults of unbalance mass and shaft crack conditions. The neural network is then trained with the generated database to automate the fault diagnostic process.

2. DESCRIPTION OF THE TEST RIG

The experimental operator is shown in Fig. 2. The experimental rotor system used in this work consisted of a motor, which was connected by a flexible coupling and a single disk rotor. The rotor shaft was supported by two identical brass bush bearings and had a length of 250 mm. The diameter of the rotor shaft was 15 mm. It had a disk of 116 mm in diameter, 22 mm in thickness and a disk of mass 1.65 kg, which were mounted on the rotor shaft mid-way between the bearing supports. The disk was fixed on the rotor shaft by radial screws. There were 36 tapped holes symmetrically placed on each side of the disk flat faces at a radius of 45 mm in order to attach any desired amount of unbalance mass. The bearing pedestals were provided in order to fix the sensors and to measure the dynamic vibration level in the horizontal, vertical and axial directions. The rotor shaft was driven by a 0.37 kW ac/dc variable speed motor. A constant operating speed of 1500 rpm was maintained, though the motor speeds ranged from 0–8000 rpm. The natural frequency of the rotor was 4.45 Hz in the lateral mode. The critical speed was 267 rpm. The piezoelectric accelerometers (Bruel and Kjaer, type 4370 piezoelectric accelerometer, charge sensitivity 9.99 picocolumbs/ms^2) were attached in three directions for measurement of RMS velocity in mm/s. The frequency analysis was carried out using a FFT analyzer (pulse lite, basic 2-channel, max 12K points up to 1000 Hz input frequency). An accelerometer enabled the measurement of the vibration level in the horizontal, vertical and axial directions. The output of the accelerometer was connected to the FFT analyzer for frequency analysis. Three special fixtures attached tightly to the bearing pedestal were used to hold the accelerometer at the desired locations. The signal was transmitted to a transducer and pre-amplifier. The output of the pre-amplifier signal was transmitted to the FFT analyzer.

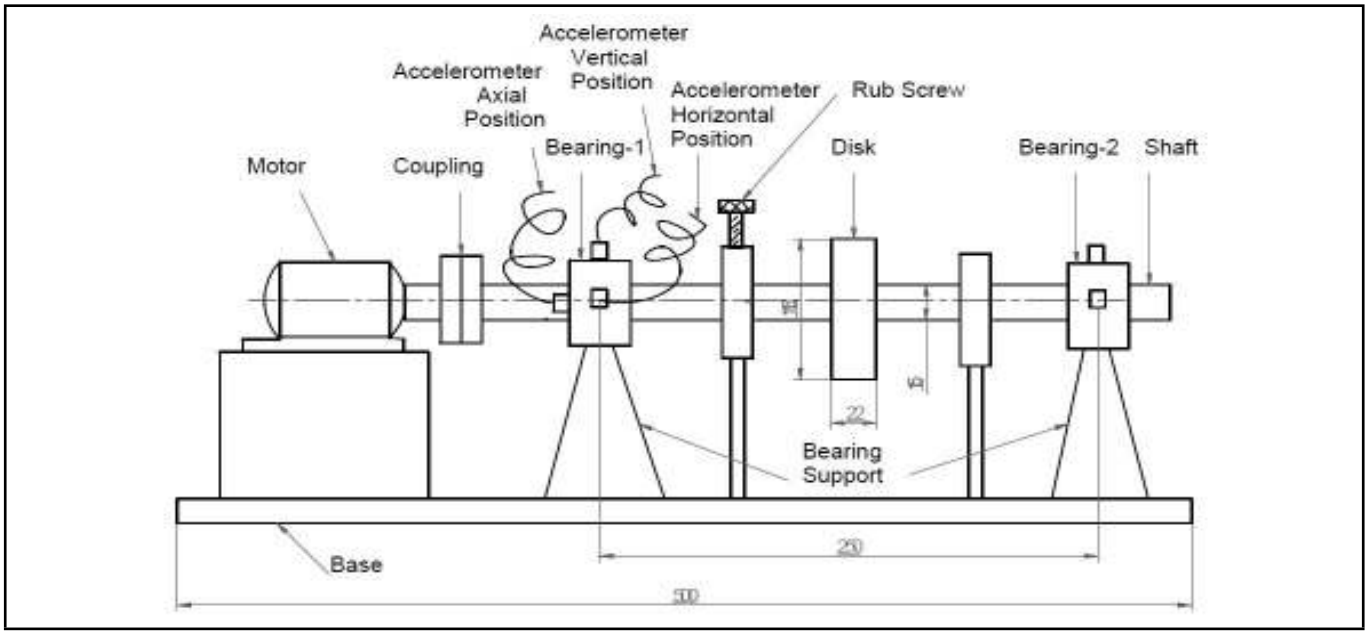

Figure 2. Rotor Test Rig.

3. FREQUENCY SPECTRUM ANALYSIS ON THE EFFECTS OF THE COMBINED FAULTS OF UNBALANCE AND SHAFT CRACK

In this experiment, combination of mass unbalance and shaft crack were both introduced simultaneously in the rotor test rig. The unbalance mass ranging from 6.5 g to 18.5 g and shaft crack ranging from 1.5 to 6.0 mm, with a combination of unbalance and shaft crack were used. The combined faults of unbalance and crack weare introduced and the vibration signals of the rotor were recorded from bearing 2 in the horizontal, vertical and axial directions. The amplitude signals are stored in a dual channel FFT analyzer for further analysis. The frequency analysis has been carried out for the frequency component of RMS velocity due to different mass unbalance and crack depths. Values of the combined faults of unbalance and shaft crack on the frequency components of the RMS velocity (mm/s) are listed in Table 1.

Initially, the base line vibration signature for "no crack" was recorded. The transverse crack with a width of 0.75 mm at a distance of 8 mm from the bearing and depth ranging from 1.5 to 6.0 mm were created at the mid span of the shaft by cutting with jewel saw. A special probe was attached to the dial indicator to measure the depth of crack. The unbalance mass range was from 6.5 g to 18.5 g with a combination of unbalance and crack. The machine was run at 1500 rpm.

It is observed that the first harmonic in the horizontal direction 1X component has increased from 0.53 mm/s to 1.98 mm/s. The second harmonic 2X has also increased from 0.046 mm/s to 0.162 mm/s. There is an increase in the level of 1X frequency component of vibration from 0.38 to 1.72 mm/s in vertical direction. The 2X frequency component of vibration has also increased from 0.039 mm/s to 0.122 mm/s in the vertical direction. It is observed from Figs. 3(a) to 3(d) that 1X frequency component of vibration is to be seen predominantly in the horizontal direction ranging from 0.53 mm/s to 1.98 mm/s for the crack depth ranging from 1.5 mm to 6.0 mm and unbalance ranging from 6.5 g to 18.5 g corresponding to a speed of 1500 rpm, and a phase angle of 48 degrees. The increase in the vibration level is the highest with 1X frequency components in the horizontal direction is 1.98 mm/s.

Table 1. Values of frequency components of the RMS vibration velocity (mm/s) for various unbalance masses ranging from 6.5 g to 18.5 g and a crack depth of 6.0 mm were obtained at a rotor speed of 1500 rpm.

Frequency Components	Training Set (mm/s) Combined Unbalance and Shaft Crack in (g/mm)			Testing Set
	6.5 6	10.5 6	14.5 6	18.5 (g) 6 (mm)
1XH	1.480	1.820	1.920	1.980
2XH	0.068	0.072	0.142	0.162
3XH	0.054	0.064	0.074	0.082
4XH	0.048	0.052	0.084	0.088
1XV	0.980	1.240	1.640	1.720
2XV	0.088	0.092	0.098	0.122
3XV	0.078	0.082	0.084	0.098
4XV	0.060	0.068	0.072	0.080
1XA	0.320	0.380	0.410	0.420
2XA	0.084	0.086	0.094	0.098
3XA	0.058	0.058	0.066	0.072
4XA	0.042	0.044	0.052	0.064

4. APPLICATIONS OF ANN FOR FAULT DIAGNOSIS

The neural network used for rotor fault diagnosis consisted of one hidden layer and one output layer. Tan-sigmoid activation function was used in the hidden layer. The output layer used a purelin transfer function. The input vectors for training the network were the RMS velocity (mm/s) frequency components of the vibration signatures measured in the horizontal, vertical and an axial direction for faults such as unbalance and crack. The network performance is called generalization, which is the ratio of actual output to the desired output expressed in a percentage. The network was trained and tested with different neuron combination with different error goals for the above faults.

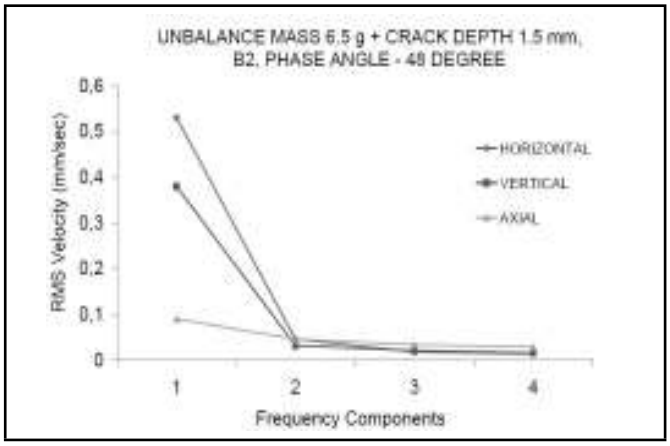

Figure 3a. Frequency components of the RMS velocity for unbalance mass of 6.5 g and a crack depth of 1.5 mm.

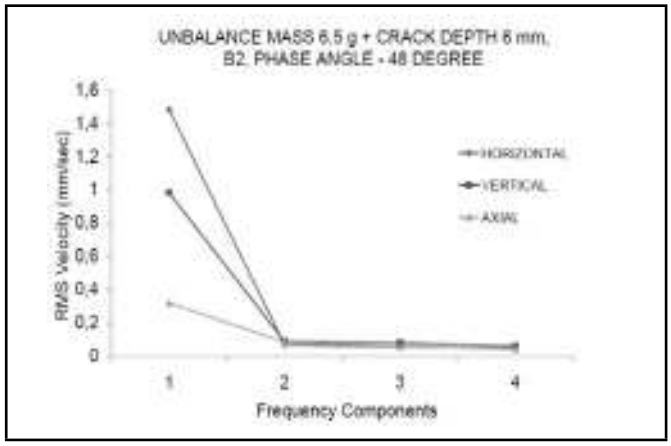

Figure 3c. Frequency components of the RMS velocity for unbalance mass of 6.5 g and a crack depth of 6.0 mm.

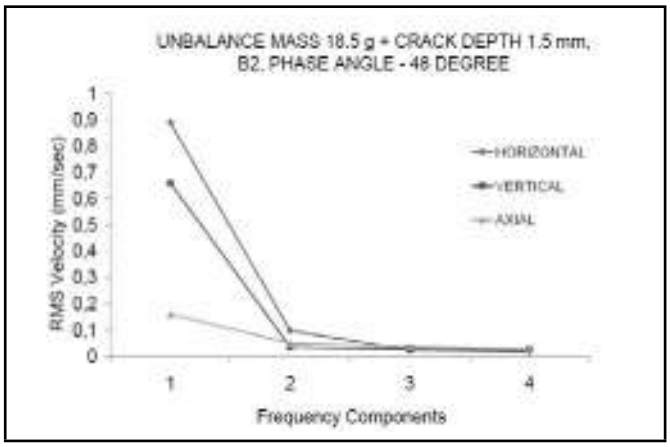

Figure 3b. Frequency components of the RMS velocity for unbalance mass of 18.5 g and a crack depth of 1.5 mm.

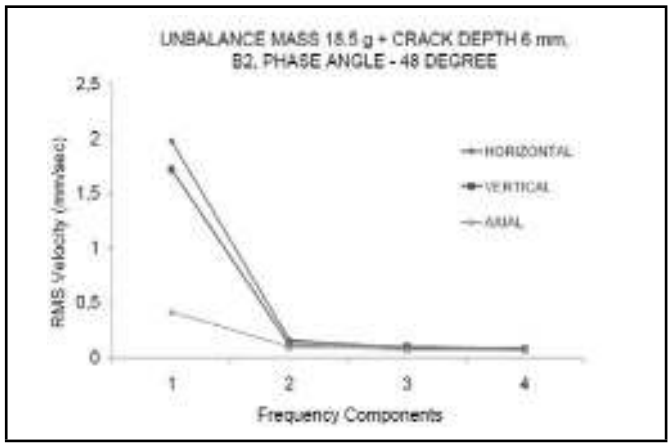

Figure 3d. Frequency components of the RMS velocity for unbalance mass of 18.5 g and a crack depth of 6.0 mm.

4.1. Network training and testing of combined faults of unbalance and shaft crack data

The training and test data of the present study were generated on a rotor test rig (shown in Fig. 2). Table 1 shows the training data and test data of the RMS velocity for various unbalance masses and crack in the horizontal, vertical, and axial directions. The values of frequency components in the horizontal, vertical and axial directions for unbalance ranging from 6.5 g to 18.5 g are noted. The ANN was trained by using MATLAB Neural Network Toolbox. The ANN is said to be trained when the epochs are maximum, learning rate μ is maximum, and error is minimum. The training was carried out using of error goals from 0.01 to 0.0001, with different numbers of neurons. Since there is no specific method to decide the exact number of neurons in the hidden layer, an empirical geometrical pyramid rule will be discussed.[3] The number of hidden neurons equals $\sqrt{mn}$, where m = number of output neurons and n = number of input neurons. In this case the value of $m = 3$, and $n = 12$. According to the empirical rule, the number of hidden neurons will be 6. The network was trained using 8 neurons with error goal combinations of 0.0001. The testing was carried out using the test set given in the last column of Table 1. From Table 1, with an error goal of 0.0001 and 8 neurons, it is seen that in training number 2, the epochs and (μ) remain constant and the sum squared error becomes minimized, which leads to a good generalization. After successful training, the network is tested for simulation with a separate set of untrained data. It is observed that the neural network is able to detect the corresponding unbalance of 18.4367 g and shaft crack of 1.4977 mm for epochs of 8 and an error of 1.81961e-007 for an error goal of 1e-005. The experimental value of unbalance is 18.5 g and the value of shaft crack is 1.5 mm. The ANN has identified the value of unbalance to an accuracy of 99.65% and shaft crack of 99.84%. This is in close correlation with the experimental values. This data is shown in Table 2.

Table 2. Quantification of unbalance mass and crack shaft, error goal 0.0001 and hidden neurons 6

Serial no.	Experimental values of combined faults of unbalance (g) and shaft crack (mm)	Epochs	MSE	ANN Quantification values	Percentage
1	6.5 1.5	3	0.00031116	6.3857 1.4971	98.24 99.80
2	18.5 1.5	8	1.81961e-007	18.4367 1.4977	99.65 99.84
3	6.5 6.0	3	0.000484793	6.4419 5.9093	99.10 98.48
4	18.5 6.0	8	3.00341e-006	18.4022 5.9957	99.47 99.92

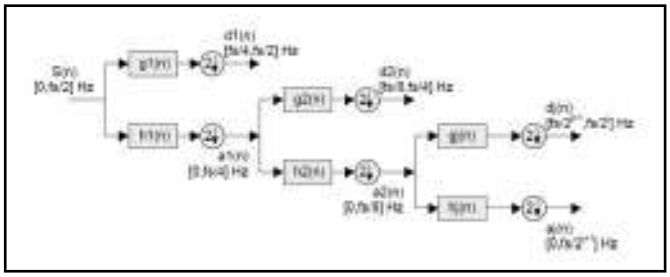

Figure 4. Multi-resolution signal decomposition.

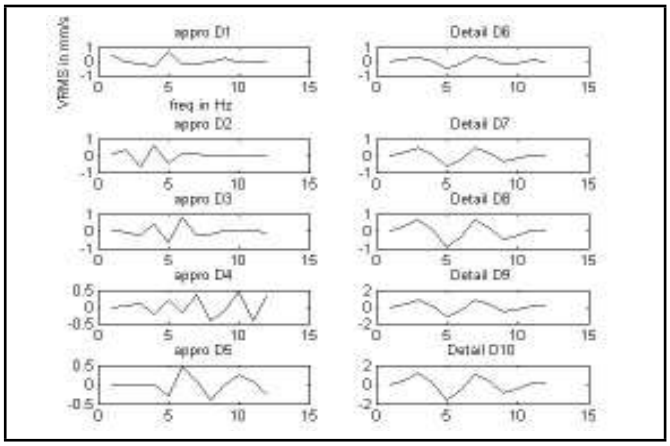

Figure 5a. Wavelet decomposition corresponding to an unbalance mass of 6.5 g and a shaft crack of 6.0 mm.

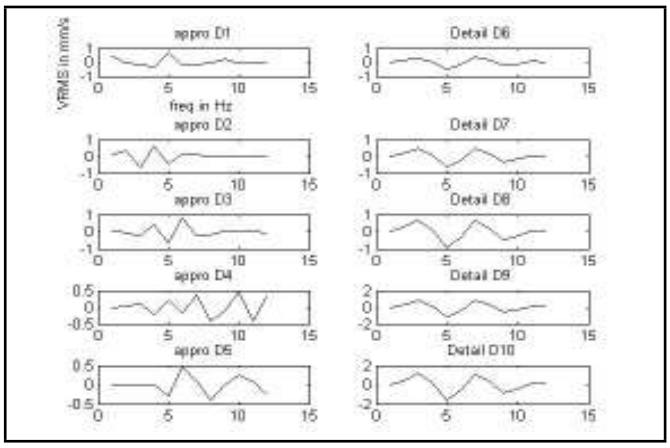

Figure 5b. Wavelet decomposition corresponding to an unbalance mass of 10.5 g and a shaft crack of 6.0 mm.

5. WAVELET ANALYSIS

Wavelet transform is a mathematical tool with a powerful structure and enormous freedom to decompose a given signal into several scales at different levels of resolution. Figure 4 shows the multi-resolution signal decomposition algorithm used for the implementation of discrete wavelet transform. In this figure, $s(n)$ is the sampled signal of $f(t)$, which is sampled at the rate of fs Hz. Then the digitized signal $s(n)$ is first decomposed into $a1(n)$ and $d1(n)$ using a low pass filter $h1(n)$, and a high pass filter $g1(n)$, respectively, where, $d1(n)$ is called the detail function, which contains higher-frequency terms, and $a1(n)$ is called the approximation signal, which contains low-frequency terms. This is called first scale decomposition. The second scale decomposition is now based on the signal $a1(n)$, which gives $a2(n)$ and $d2(n)$. The next higher

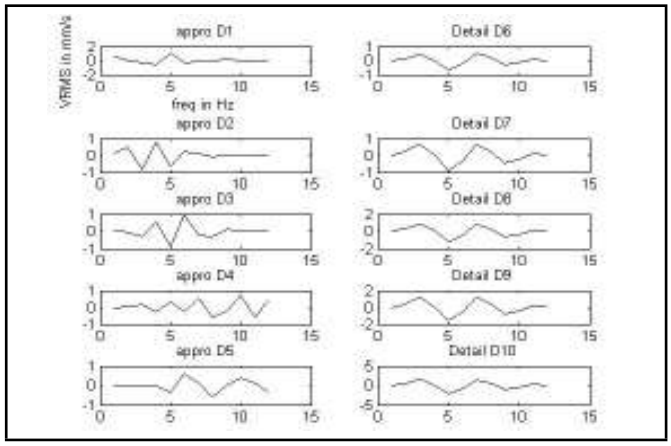

Figure 5c. Wavelet decomposition corresponding to an unbalance mass of 14.5 g and a shaft crack of 6.0 mm.

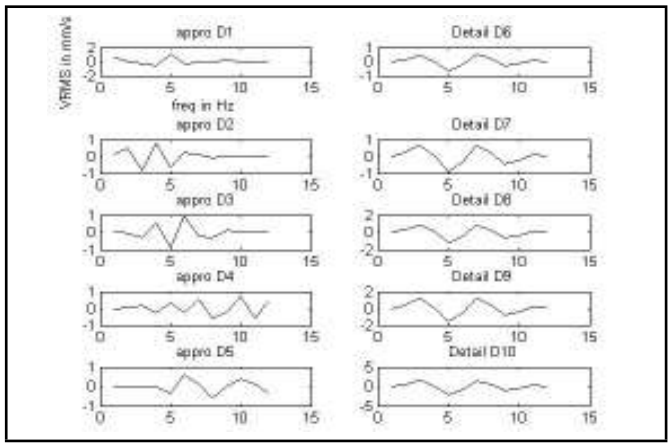

Figure 5d. Wavelet decomposition corresponding to an unbalance mass of 18.5 g and a shaft crack of 6.0 mm.

scale decomposition is now based on $a2(n)$ and so on. At any level f the approximation signal $aj(n)$ will be composed of frequencies 0–f_c Hz. Similarly, the detail signal $dj(n)$ at any level f will contain frequencies of range f_c–2 Hz. The cutoff frequency f_c of approximation signal $aj(n)$ for a given level f is found by

$$f_c = \frac{f_s}{2^{f+1}}. \tag{3}$$

Additionally, the number of points in the decomposed detail and approximation signals decreases gradually through successive decimation. Thus, to compute the discrete wavelet transform (DWT) all that is needed are filters. The signal is convolved with these filters. In contrast to the short-time Fourier transforms (STFT), the time resolution becomes arbitrarily fine at high frequencies, while the frequency resolution becomes arbitrarily fine at low frequencies. In the present work, an attempt was made to use wavelet transform for identification of rotor fault, which does not depend on a single frequency, but on a band of frequencies.

5.1. Feature Extraction

The aim of the feature extraction is to apply the transformation that extracts the signal features hidden in the original frequency domain. Corresponding to different characteristics of the signal, transformation should be properly selected so

Table 3. RMS value of vibration signal and its ten detailed coefficient wavelet decompositions

Unbalance Mass (g) + Shaft Crack (mm)	Original RMS	D1	D2	D3	D4	D5	D6	D7	D8	D9	D10
Unbalance Mass 6.5 g + Shaft Crack 6.0 mm	0.4432	0.2541	0.3296	0.3996	0.2747	0.1762	0.1973	0.3495	0.6314	1.0864	1.9250
Unbalance Mass 10.5 g + Shaft Crack 6.0 mm	0.6940	0.4064	0.5050	0.6013	0.4282	0.2700	0.3026	0.5359	0.9677	1.6653	2.9507
Unbalance Mass 14.5 g + Shaft Crack 6.0 mm	1.5622	0.6322	0.5712	0.6111	0.6027	0.3169	0.3501	0.6220	1.1159	1.9228	3.4061
Unbalance Mass 18.5 g + Shaft Crack 6.0 mm	3.3088	0.6834	0.6037	0.6443	0.6473	0.3345	0.3696	0.6560	1.1770	2.0279	**3.5923**

Table 4. Normalized training data set

SI. No	Unbalance Mass + Shaft Bow	Input									
		W1	W2	W3	W4	W5	W6	W7	W8	W9	W10
1	Unbalance Mass 6.5 g + Shaft Crack 6.0 mm	0.1389	0.1490	0.1593	0.1407	0.1261	0.1292	0.1518	0.1937	0.2612	0.3860
2	Unbalance Mass 10.5 g + Shaft Crack 6.0 mm	0.1603	0.1750	0.1893	0.1640	0.1400	0.1450	0.1796	0.2440	0.3472	0.5380
3	Unbalance Mass 14.5 g + Shaft Crack 6.0 mm	0.1940	0.1850	0.1907	0.1894	0.1470	0.1520	0.1924	0.2660	0.3854	0.6056
4	Unbalance Mass 18.5 g + Shaft Crack 6.0 mm	0.2015	0.1896	0.1960	0.1962	0.1496	0.1550	0.1980	0.2750	0.4010	0.6334

that the specific signal structure can be enhanced in its transformed domain. The fault identification techniques are those which compare the current data with that of the known cases to reach a final diagnosis. A multi-resolution property of the discrete wavelet transform (DWT) is used to analyze the vibration signal under different fault conditions. The Daubechies wavelet was selected for the signal analysis because it provides a much more effective wavelet than that obtained with the other wavelets (Haar, Coifman, etc). When vibration signals collected under different conditions are decomposed via the wavelet, the appreciable differences between the corresponding wavelet coefficients, as shown in Figs. 5(a),(b),(c), and (d), can be seen. However, conducting a direct assessment from all wavelet coefficients turns out to be tedious job. Therefore, the wavelet node power ej at f level decomposition in defined as $ej = 1/Nj$.

Here, Nj is the number of coefficients at level f, wj, k is the k^{th} coefficient calculated for j^{th} level, ej is the RMS (root mean square) value of the decomposed signal at a level f. It measures the signal power contained in the specified frequency band indexed by the parameter f in order to relate the RMS value of the wavelet decomposition signals with different rotor faults. For each case four sets of data are recorded.

The vibration in the RMS value of the first ten decompositions for one segment from each case is shown in Table 3. The similar values are obtained for other vibration segments. From Table 1, it is clearly observed that the shaft crack depth is kept at a constant 6.0 mm, and the unbalance mass is varies from 6.5 g to 18.5 g in order to study the vibration characteristics due to the combination of unbalance and shaft crack. Due to an increase of unbalance mass with a constant crack depth, the 1X frequency component of the RMS velocity is predominant in the horizontal direction.

5.2. Data Normalization

During the training of the neural network, input variables of higher values may tend to suppress the influence of the smaller one. To overcome this problem and in order to make neural network perform well, the data must be well processed and properly scaled before being input into the ANN. All the components of the feature vector are normalized using the equation

$$x_n = \left[\frac{x}{1.5 \times x_{max}}\right] 0.8 + 0.1, \tag{4}$$

where x is actual data, x_{max} is the maximum value of the data, and x_n is the normalized data. The maximum value is obtained from the faulty data set. The maximum value is multiplied by the factor 1.5 so that if the fault severity is more than what is considered until now, the same neural network can be useful for fault identification. Table 4 shows the normalized value of the RMS level given in Table 3 by using Eq. (4). The neural network toolbox of MATLAB has been used to simulate the desired network. The "newff" function of MATLAB has been used to create a three-layered back propagation network. In the training process, the network is trained according to the Levenberg-Marquardt optimization technique until the mean square error is found below 0.0001 or the maximum number of epoch's (300) is reached.

Table 4 shows the normalized values of wavelets of combined faults of unbalance and shaft crack. The first three rows of data [(6.5g+6.0mm) to (14.5g+6.0mm)] have been used for training the network and the last row of data (18.5g to 6.0mm) is test data. The network has used 6 neurons with error goal of 0.0001. The testing set has been shown in the last row of Table 4. After sum squared error has decreased and μ has increased it yielded good generalization. Using this network the combined faults of unbalance and shaft crack has been quantified as 18.4998 g and 6.0 mm or 99.99 % and 100.00 % of the experimental value. The result as shown in Table 5.

6. CONCLUSIONS

The amplitude of vibration of a rotor bearing system, which is measured in the horizontal, vertical and axial directions, is used to study the effects of vibration characteristics of a combination of unbalance and shaft crack. The experiments are carried out by creating a crack depth ranging from 1.5 mm to 6.0 mm by varying the unbalance mass. It is recorded that the 1X frequency component of vibration has predominantly increased in the horizontal direction in all of the cases. To

Table 5. Quantification of combined faults of unbalance and shaft crack using combined form of ANN and wavelet transform, error goal of 0.0001 and hidden neurons 6

Serial no.	Experimental values of combined faults of unbalance (g) and shaft crack (mm)	Epochs	MSE	Combined ANN and wavelet transform Quantification values	Percentage
1	6.5 6.0	3	1.21179e-007	6.4998 5.9996	99.99 99.99
2	10.5 6.0	8	0.000971871	10.4995 6.0000	99.99 100.00
3	14.5 6.0	5	8.88666e-006	14.4998 5.9998	99.99 99.99
4	18.5 6.0	4	0.000357918	18.4998 6.0000	99.99 100.00

quantify these faults, one promising approach is to use the artificial neural network of a multilayer feed forward back propagation algorithm. It has been seen by training of network with data that was obtained experimentally and by testing the same data. Further work needs to be done by using other types of networks and algorithms. Removing the arbitrariness in the choice of the network parameters is another area where more work must be done. The ANN is used for diagnosing and quantifying of faults. The success rates, based upon each fault, have been reported .In particular, overall success rates of 99.78% for unbalance, 99.81% for shaft crack, and 99.45% for the combined faults of unbalance and shaft crack have been achieved. This paper has also investigated the feasibility of applying the discrete wavelet transform to identify the combined faults of unbalance mass and shaft crack. To alleviate the frequency-invariant characteristics of the wavelet coefficients and to reduce the dimensionality of the input to the neural network, the RMS value at selected decomposition levels are used as a feature measure of the signal. The features obtained by the proposed method yields nearly 99.99% quantification when used as input to a neural network.

REFERENCES

[1] Dutt, J. K. and Nakra, B. C., Stability of rotor system with viscoelastic support, *Journal of Sound and Vibration*, **153**(1), 89–96, (1993).

[2] Genta, G. and De Bona, F., Unbalance response of rotors; A modal approach with some extensions to damped natural systems , *Journal of Sound and Vibration*, **140**(1), 129–153, (1990).

[3] Edwards, S., Lees, A. W., and Friswell, M. I., Fault diagnosis of rotating machinery, *The Shock and Vibration Digest*, **30**(1), 4–13, (1998).

[4] Gasch, R., A survey of the dynamic behavior of a simple rotating shaft with a transverse crack, *Journal of Sound and Vibration*, **160**(2), 313–332, (1993).

[5] Meng, G. and Hahn, E. J., Dynamic response of cracked rotor with some comments on crack detection, *Journal of Engineering for Gas Turbines and Power*, **119**(2), 447–455, (1997).

[6] Isermann, R., Supervision, fault detection and fault-diagnosis methods, *Control Engineering Practice*, **5**(5), 639–652, (1997).

[7] Lees, A. W. and Friswell, M. I., The evaluation of rotor imbalance in flexibly mounted machines, *Journal of Sound and Vibration*, **208**(5), 671–683, (1997).

[8] Hall, D. L., Hansen R. J., and Lang, D. C., The negative information problem in mechanical diagnostics, *Journal of Engineering for Gas Turbines and Power*, **119**, 370–377, (1997).

[9] Srinivasan, K. S., Fault diagnosis in rotating machines using vibration monitoring and artificial neural networks, Ph. D Thesis ITMMEC, Indian Institute of Technology Delhi, (2003).

[10] Srinivasan, K. S. and Umesh, K. N., Study of effects of misalignment on vibration signatures of rotating machinery, National Conf. README-05, PACE, Mangalore, (2005).

[11] McCormick, A. C. and Nandi, A. K., A comparison of artificial neural networks and other statistical methods for rotating machine condition classification, IEEE, Savoy London, 2(1)–2(6), (1996).

[12] McCormick, A. C. and Nandi, A. K., Classification of the rotating machine condition using artificial neural networks, *Proceedings Instrumentation Mechanical Engineers*, **211**(C), 439–450, (1997).

[13] Vyas, N. S. and Kumar, D. S., Artificial neural network design for fault identification in rotor-bearing system, *Mechanism and Machine Theory*, **36**, 157–175, (2001).

[14] Kalkat, M., Yildirim, S., and Uzmay, I., Rotor dynamics analysis of rotating machine systems using artificial neural networks, *International Journal of Rotating Machinery*, **9**, 255–262, (2003)

[15] Nahvi, H. and Esfahanian, M., Fault identification in rotating machine condition using artificial neural networks, *Proceedings Instrumentation Mechanical Engineering Science*, **219**(2), 141–158, (2004).

[16] Ryu, J. S., Yoon, D. B., and Wu, J. S., Development of a HANARO vibration monitoring system for rotating machinery, Proceedings of the Internal Symposium on Research Reactor and Neutron Science, (2005).

[17] Chow, T. S. W. and Jaw, L. T., Rotating machines fault identification using back-propagation artificial neural network, City Polytechnic of Hong Kong, 405–412.

[18] Yen, G. G. and Lin, K. C., Wavelet packet feature extraction for vibration monitoring, *IEEE Transactions on Industrial Electronics*, **47**(3), 650–666, (2000).

[19] Boras, D., Castila, M., Moreno, N., and Montano, J. C., Wavelet and neural structure: A new tool for diagnostic of power system disturbances, *IEEE Transactions on Industry Applications*, **37**(1), 184–190, (2001).